



How do fronts affect phytoplankton communities over oceanic regions ? Contrasting responses across trophic regimes, seasons and front diagnostics

Angelina Cassianides¹, Marina Levy¹, Clément Haëck¹, Ines Mangolte², Roy El Hourany³, Michela Sammartino⁴, and Bruno Buongiorno Nardelli⁴

¹LOCEAN-IPSL, Sorbonne Université, CNRS, IRD, MNHN, Paris, France

²ENTROPIE, IRD, CNRS, UR, UNC, Ifremer, Noumea, New Caledonia

³LOG, Univ. Littoral Côte d'Opale, Univ. Lille, CNRS, IRD, Wimereux, France

⁴Consiglio Nazionale delle Ricerche, Istituto di Scienze Marine (CNR-ISMAR), 80133, Naples, Italy

Correspondence: Angelina Cassianides (angelina.cassianides@locean.ipsl.fr)

Abstract.

Oceanic fronts are key features structuring marine ecosystems, yet their influence on phytoplankton communities remains difficult to quantify at regional scale. In particular, how phytoplankton responses to fronts vary across environmental conditions is still poorly understood, and may depend on the way fronts are detected. Here, we investigate how fronts affect phytoplankton biomass and community composition across the Mediterranean Sea, a region characterized by strong seasonal variability and contrasted trophic regimes. Using 23 years (1998–2021) of satellite-derived chlorophyll-a and pigment-derived phytoplankton groups data, we quantify phytoplankton responses to fronts across seasons and biogeochemical provinces, from productive northwestern regions to ultra-oligotrophic eastern basins. Fronts are identified using either the measure of an heterogeneity index (HI) or of Finite-Size Lyapunov Exponents (FSLE), applied, in both cases, to different data sources (satellite data or high-resolution fields reconstructed from machine-learning). This approach allows us to assess the sensibility of observed ecological responses to the choice of front detection method. We show that fronts are consistently associated with enhanced phytoplankton biomass by 4% to 35% and reshaped community composition across the Mediterranean Sea, with the strongest effects observed in oligotrophic regimes and during stratified periods. In particular, fronts are associated with an enrichment in diatoms by up to 20% and a relative decrease in prokaryotes, suggesting enhanced nutrient supply. However, the magnitude and consistency of these responses vary depending on the diagnostic used, with weaker to no signals detected using FSLEs. These results demonstrate that phytoplankton responses to fronts are both environmentally controlled and method-dependent. They highlight the key role of fronts in structuring ecosystems in nutrient-limited regions, and support the idea that changes in oceanic fronts should be considered when investigating ecological reorganization under future climate change scenarios, particularly in climate change hotspots such as the Mediterranean Sea.



20 1 Introduction

Phytoplankton are fundamental for the functioning of the oceans, by supporting marine ecosystems and regulating biogeochemical cycles. Biogeochemical cycles and the dynamics of marine food webs are directly influenced by the diversity and composition of phytoplankton community structures. Understanding what governs phytoplankton abundance and diversity is therefore essential. Oceanic fronts are well-known to be hotspots for primary production and marine ecosystems: they can supply nutrients that stimulate phytoplankton growth (Lévy et al., 2015; Mahadevan, 2016), reorganize phytoplankton communities (d'Ovidio et al., 2004; Lévy et al., 2018; Tzortzis et al., 2021), modulate light availability and restratification (Lévy et al., 2018; McKee et al., 2023), reshape ecosystems (Lévy et al., 2018), constitute habitats to higher trophic levels including fishes, marine mammals and sea birds (Bost et al., 2009; Siegelman et al., 2019; Baudena et al., 2021) and have implications for fishing strategies (Watson et al., 2018).

Oceanic fronts are fundamentally associated with lateral density gradients, which drive along-front geostrophic currents and across-front ageostrophic secondary circulation, including vertical motions that can strongly influence phytoplankton dynamics (e.g., Lévy et al., 2018). They are ubiquitous features observed everywhere in the ocean, with quite variable characteristics. Their spatial scale spans a large range, from a few hundred meters to hundreds of kilometers in length. Some fronts are permanent features, such as the Gulf Stream (Thomas et al., 2016), while others are more seasonal (Sudre et al., 2023a) or ephemeral, persisting for only days or weeks. Some fronts are associated with large density gradients (D'Asaro et al., 2011), others with weaker ones (Haëck et al., 2023). Most fronts display signatures in both sea surface temperature (SST) and density and are also detectable through their surface physical dynamics, an along front current (Sudre et al., 2023b). Such fronts are generally associated with intense vertical velocities. However, sometimes, thermohaline compensation occurs, and SST gradients are not associated with strong density gradients, in such cases, vertical motions are much weaker or even absent (e.g., Mauzole et al., 2020). Besides, density fronts can extend from just a few meters within the mixed layer (Fox-Kemper et al., 2008) to depths, reaching up to 1000 m (Siegelman et al., 2020; Sudre et al., 2023a) thereby having different influence on oceanic vertical transport and nutrient supply (Lévy et al., 2018).

Investigating fronts has been largely facilitated by the acquisition of SST satellite images, either using thresholding of SST gradients (e.g., Belkin and O'Reilly, 2009), histogram analysis (e.g., Cayula and Cornillon, 1992), deep learning (Li et al., 2022) or SST heterogeneity (Liu and Levine, 2016; Haëck et al., 2023). Fronts can also be detected using lagrangian diagnostics from altimetric currents, such as Finite-Size Lyapunov Exponents (FSLEs) which characterize strain fields and identify regions where fluid motion undergo strong stretching (d'Ovidio et al., 2004; Hernández-Carrasco et al., 2011; Sudre et al., 2023b). Importantly, these different approaches provide different diagnostics of the same underlying physical structures, with distinct sensitivities and limitations. Typically, the SST heterogeneity method has the advantage to be applied to kilometric resolution data (such as satellite SST) which are very precise but sometimes lacking due to cloud cover. Also, it captures SST and not density fronts, and therefore might overestimate the presence of dynamically active fronts. On the other hand, the FSLE method provides a more continuous description of fronts, but based on coarser resolution satellite sea-surface high data, which can lead to potential misalignment of the actual front position by a few tens of kilometers (e.g., Lehahn et al., 2007).



Advances in observational and detectable methods has significantly improved our ability to quantify oceanic fronts influence
55 on phytoplankton abundance and community structure over wide ocean regions (Liu and Levine, 2016; Haëck et al., 2023;
Lévy et al., 2025). These studies were focused on the tropical Pacific and North Atlantic, and used SST heterogeneities to
detect fronts. Other studies have also highlighted Chl-a convergence along FSLE filaments in the Western Mediterranean Sea
(Hernández-Carrasco and Orfila, 2018; Hernández-Carrasco et al., 2020; Tzortzis et al., 2021).

Our main objective is to quantify the changes in phytoplankton biomass and composition in response to fine scale fronts
60 in the Mediterranean Sea. We aim to determine how fronts affect phytoplankton communities across seasons and trophic
regimes, and to assess the robustness of these responses using different front detection diagnostics. While often considered to
be an oligotrophic basin, the Mediterranean Sea is in fact characterized by a mosaic of bioregions with extremely contrasted
biogeochemical conditions, from the highly productive Gulf of Lion to the ultra-oligotrophic Ionian-Levantine basin (Figure 1,
Siokou-Frangou et al. (2010)). This diversity of biogeochemical conditions offers a unique opportunity to evaluate the impact
65 of fronts across a wide range of environments. In addition, the Mediterranean Sea exhibits strong seasonal variability, making
it particularly suitable to investigate how phytoplankton–front interactions evolve across seasons and trophic regimes. Fronts
are ubiquitous features in the Mediterranean Sea (e.g., Hernández-Carrasco et al., 2020; Barral et al., 2021; Sudre et al.,
2023b; Akpınar, 2024), detected by thermal gradients or FSLE (Sudre et al., 2023b). Several case studies have shown local
phytoplankton enrichments at frontal scale (Olita et al., 2014; Ruiz et al., 2019; Hernández-Carrasco et al., 2020; Tzortzis
70 et al., 2021), shaping of the phytoplankton landscape by frontal boundaries (d’Ovidio et al., 2004), and fronts serving as habitat
for specific communities (Hernández-Carrasco et al., 2020; Tzortzis et al., 2023; Oms et al., 2026). However, these studies
were generally restricted to specific events lying on ship-based observation (Hernández-Carrasco et al., 2020; Tzortzis et al.,
2021; Oms et al., 2026), multiplatforms observation (Ruiz et al., 2019), or gliders (Olita et al., 2014), too scarce to provide a
quantification of frontal effects on phytoplankton at the regional scale.

75 **2 Data and Methods**

To detect fronts, we applied two methods : the Heterogeneity Index (HI) algorithm and FSLEs diagnostics. We first applied
these methods to 23 years (1998-2021) of satellite data (SST for HI and SSH for FSLEs). Then we applied them to high-
resolution density (for HI) and velocity fields (for FSLEs), reconstructed over 6 years (2016-2021, 4DMed-Sea project, Sam-
martino et al., 2025). We also used satellite data of Chl-a and pigment-derived phytoplankton groups, over 23 years, to quantify
80 the impact of fronts on phytoplankton based on the Chl-a excess and the anomaly of phytoplankton groups over fronts. This
quantification is conducted seasonally, to capture the pronounced seasonality in Chl-a (Siokou-Frangou et al., 2010) and in
fine scale front dynamics (Hernández-Carrasco and Orfila, 2018; Akpınar, 2024) of the Mediterranean Sea. It is also conducted
regionally to contextualize interactions under regionally coherent physical and biogeochemical conditions. Our methodological
choices allow us to quantify phytoplankton responses to fronts across contrasting environmental conditions, and to assess how
85 these responses depend on both environmental variability and the diagnostic used to detect fronts.



2.1 Data

For SST, we used the European Space Agency Sea Surface Temperature Climate Change Initiative (ESA SST CCI) and Copernicus Climate Change Service (C3S) level 4 analysis product. The SST field is created with Operational SST and Sea Ice Analysis (OSTIA, Good et al., 2020) combining data from different infrared sensors ((A)ATSR, SLSTR, and AVHRR sensors, Merchant et al., 2019). The SST CCI covers the period from 1st September 1981 to 31st December 2016, and the C3S data from 1st January 2017 onwards. To coincide with the period of availability of Chl-a data, we use SST data between 1998 to 2021, daily, with a resolution of $1/20^\circ$. In order to generate a cloud-free product, a spatial interpolation is applied where SST are unavailable. While this approach ensures comprehensive coverage across the studied area, the interpolation leads to an underestimation of front detection due to the smoother SST field over regions covered by clouds. Nevertheless, using multiple sensors serves to minimise the extent of these areas.

Density fields are available for the entire Mediterranean basin, on a regular grid with a spatial resolution of $1/24^\circ$, and a time interval of 1 day from 1st January 2016 to 1st August 2022. These data take part of the 4DMed-Sea project, which aims to use Machine Learning algorithm to reconstruct vertically several parameters such as density, from the surface across 148 verticals levels from 3m to 150 m depth, with a step interval of 1m (4DMed-Sea project, Sammartino et al., 2025). In our case study, we focused solely on surface data obtained through a multivariate optimal interpolation algorithm, that combines satellite UHR SST data and sea surface salinity images from various satellites sources and in situ measurements (Sammartino et al., 2022). These density fields provide a more direct representation of frontal density gradients and allow us to identify dynamically relevant fronts.

We used the daily FSLE product distributed by AVISO, derived from the SSALTO/Duacs delayed-time global ocean absolute geostrophic currents a resolution of $1/4^\circ$. FSLE are computed backward-in-time, in order to measure the separation rate of initially contiguous particles, with the initial separation fixed as 0.02° and the final separation as 0.6° . They are available over the period 1998–2021, with a spatial resolution of $1/25^\circ$ (d’Ovidio et al., 2004). We also used the FSLE data developed in the 4DMED-SEA project, derived from velocity fields with a finer grid in order to investigate whether the spatial resolution of products can influence our quantification (Cortés-Morales and Hernández-Carrasco, 2024). These FSLEs are derived from reconstructed geostrophic currents, using the 4DVARNET algorithm (Fablet et al., 2021), at a resolution of $1/24^\circ$. The initial distance δ_0 separating the particles is set at $1/24^\circ$, the final separation is set to $\delta_f = \delta_0 * \alpha$ with $\alpha = 30$ (Hernández-Carrasco et al., 2011). The 4DMED-FSLE are daily from April 2016 to July 2022, with a horizontal resolution of $1/24^\circ$.

For Chl-a data, we used the L3 product provided by ACRI-ST over the period 1998–2021, based on the Copernicus-GlobColour processor. It is obtained by merging and reprocessing data from different sensors (SeaWiFS, MODIS Aqua & Terra, MERIS, VIIRS-SNPP & JPSS1, OLCI-S3A & S3B). Data are daily and available at 4 km resolution (Garnesson et al., 2019).

To retrieve phytoplanktonic taxonomic groups we used the algorithm developed by Hourany et al. (2019), which estimates nine secondary phytoplankton pigments from satellite remote sensing reflectances at different wavelengths, along with SST and Chl-a, using a neural network classifier. It provides the relative abundances of six distinct eukaryotic groups (diatoms,



120 dinoflagellates, haptophytes, green algae, cryptophytes, and pelagophytes) and one prokaryotic group, available daily at a 4 km resolution from 1998 to 2021. We merged the five non-diatom eukaryotic groups (dinoflagellates, haptophytes, green algae, cryptophytes, and pelagophytes) into a single category, as their share common variabilities and distributions. We then focused our analysis on three primary categories: diatoms, other eukaryotes, and prokaryotes.

2.2 Method

125 2.2.1 Regionalisation

The Mediterranean Sea is characterized by complex biogeochemical conditions featuring both highly productive region, such as the intense spring bloom in the Gulf of Lion, and oligotrophic areas, particularly in the Ionian and Levantine basins. Besides, several studies have highlighted the complex submesoscale and mesoscale circulation within the basin. These include the propagation of numerous eddies (Millot, 1991; Hernández-Carrasco et al., 2011; Pegliasco et al., 2021), the formation of jets
130 in specific sub-basins (Renault et al., 2012; Sala et al., 2022) and the development of filaments and frontal areas (Hernández-Carrasco et al., 2020; Barral et al., 2021; Sudre et al., 2023b).

To recontextualize the effect of fronts to phytoplankton considering the biogeochemical and physical complexity of the Mediterranean Sea, we divided the basin into four regions (Figure 1b) using a semi-automatic regionalization method. Initially, we used the regionalization of Hourany et al. (2021), based on a self-organizing classification, combining SST, mixed layer
135 depth and Chl-a data to identify seven regions, each characterized by distinct physical and biogeochemical characteristics. Then, we simplified this clustering to delineate four large and homogeneous regions, identified as: the Alboran basin (light blue), the Gulf of Lion (green), the Algerian and Tyrrhenian basins (yellow) and the Ionian and Levantine basins (orange). In contrast to Hourany et al. (2021), we excluded the Adriatic and Aegean basins as well as the coastal regions where phytoplankton biomass is predominantly influenced by river runoff and continental shelf dynamics, thereby pixels where water depth is
140 less than 100m are excluded.

The Alboran Sea (in light blue on Figure 1b) is one of the most productive regions within the Mediterranean Sea (Lazzari et al., 2011), sustained by an upwelling forced by the wind (Mercado et al., 2012) and the Atlantic Jet (Macías et al., 2008). The dynamical circulation consists of two coherent anticyclonic gyres and is characterized by strong density gradients resulting from the contrast between the saltier warmer waters of the Mediterranean Sea and the incoming fresher, cold inflows from the
145 Atlantic Ocean. In the northwestern Mediterranean Sea (green region on Figure 1b), phytoplankton seasonality is similar to temperate regions characterized by a pronounced spring bloom, summer oligotrophy, and a secondary autumn bloom (Siokou-Frangou et al., 2010; Mayot et al., 2017). The spring bloom is primarily driven by winter deep convection, which is induced by atmospheric forcing (Lévy et al., 1998; Heimbürger et al., 2013; Severin et al., 2017). The Algerian-Tyrrhenian basins and the Ionian-Levantine basins are the largest regions with ultra-oligotrophic conditions persisting throughout the year (Uitz
150 et al., 2012). Numerous eddies propagate in the Algerian-Tyrrhenian area, which coexist with quasi-permanent structures such as a wind-driven gyre in the North Tyrrhenian Sea and the Rhodes gyre. The Ionian-Levantine basin is characterized by elevated SST with a circulation pattern marked by the Ierapetra Gyre, located southeast of Crete. Figure 1c shows that other

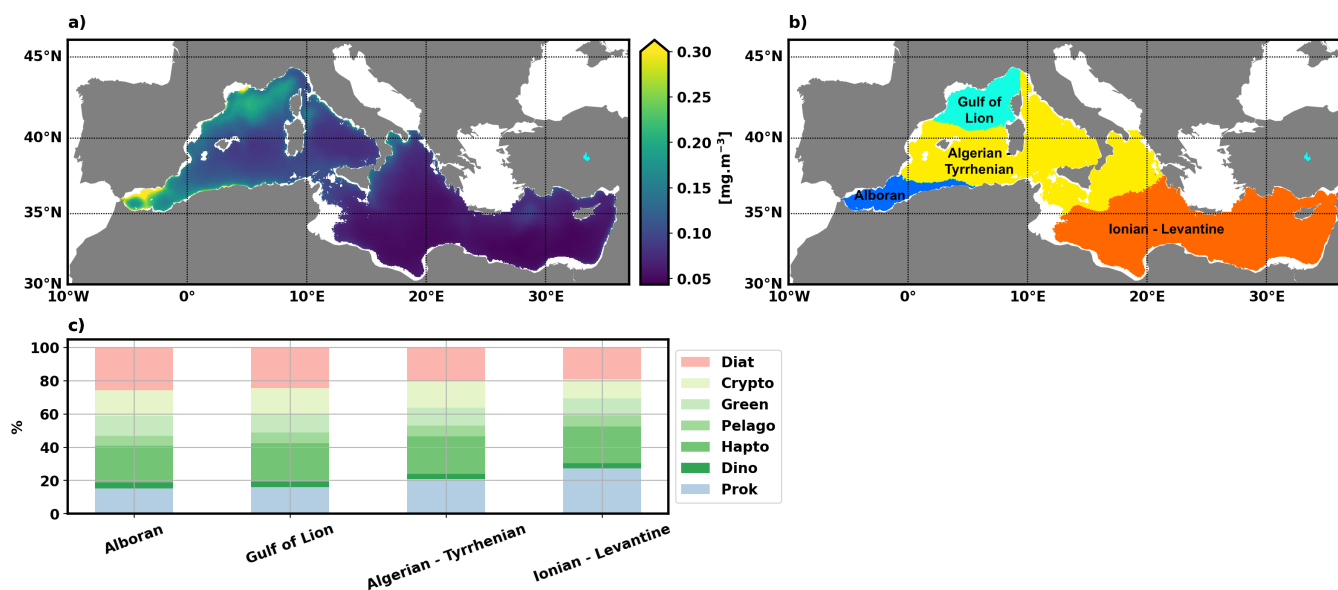


Figure 1. Overview of the study domain. (a) Time-mean of Chl-a from remote sensing over 1998-2021. (b) Regionalisation of the Mediterranean sea into four bio-regions. (c) Time-mean of phytoplankton assemblages from pigment-derived phytoplankton groups data.

eukaryotes are the dominant group basin-wide, reflecting the oligotrophic conditions, while studies highlighted the emergence of a phytoplanktonic groups mosaic at finer spatial and temporal scales (Siokou-Frangou et al., 2010).

155 2.2.2 Front detection

We detected fronts using two diagnostics (HI and FSLE) in order to compare how each method captures frontal structures associated with phytoplankton variability. To enable comparison between diagnostics, all fronts are projected onto a common grid and analyzed using a consistent statistical framework. Differences in data sources, spatial resolution and temporal coverage are taken into account when interpreting phytoplankton responses.

160 Fronts detected using HI

We used the method described by Haëck et al. (2023), inspired by Liu and Levine (2016). This method implies to compute the heterogeneity of SST (or density), and to assume that larger heterogeneities are associated with the presence of fronts. The heterogeneity can be described by three statistical metrics the bimodality, the standard deviation and the skewness. These three metrics are then combined into a single index named Heterogeneity Index (HI). This method identifies fronts as regions of enhanced horizontal gradients and spatial heterogeneity in SST (or density) fields.

The process started by sorting the domain into pixels. A moving window was then applied, of 7×7 pixels, centered on a pixel. This limited the computation of the three components and HI to a 28 km square window in order to quantify the heterogeneity for structures smaller than 28 km, and larger than 10 km. In the Mediterranean Sea, the Rossby deformation radius ranges from 10 to 15 km (Capó et al., 2019). Thus, this window size captured the signature of fine scale fronts and eddy



170 edges. We conducted sensitivity tests by varying the window size (3×3 pixels and 5×5 pixels) to confirm that the 7×7 pixels window was the most optimized choice for our study.

HI is the weighted sum of the skewness γ , the standard deviation σ , and bimodality B of SST density, defined as : $HI = a(b\gamma + c\sigma + dB)$, with a, b, c, d constant normalization coefficients. b, c, d are defined as the inverse of the standard deviation of each component, calculated over one year. The bimodality B is defined as the L2 norm of the difference between the SST
175 histogram and a Gaussian fit of the histogram. Each component is normalized by its variance. Then, HI is normalized by the coefficient a , so that 95% of the values are below an arbitrary value of 9.5.

We finally defined pixels with small heterogeneity referred to as background circulation ($HI < 10$) and pixels with large heterogeneity as fronts ($HI > 10$).

Fronts detected using FSLE

180 FSLEs identify regions of strong horizontal stretching in the flow and are widely used to detect frontal structures and transport barriers. We defined pixels with small FSLE intensity as the background circulation $FSLE < 0.17$ and pixels with large FSLE intensity as fronts $FSLE > 0.17$. Our choice of the threshold is based on a comparison with previous studies (d'Ovidio et al., 2004; García-Olivares et al., 2007; Sudre et al., 2023b) and sensitivity tests we conducted, which guided us toward this optimal value. Because standard (AVISO-based) FSLE fields are derived from altimetric currents, their effective spatial
185 resolution may limit their ability to accurately localize fine scale frontal structures. To assess whether the coarse resolution of AVISO currents to compute FSLEs influences our quantification, we compared our results using AVISO-FSLEs with FSLEs computed with higher resolution velocities (4DMED-FSLEs).

2.2.3 Quantification of the impact of fronts on phytoplankton

Our main objective is to quantify the effect of fronts on phytoplankton biomass for each region and for each season. Thus,
190 we want to compare the value of Chl-a over fronts to the regional value. For each day, we collocated Chl-a data with front positions (identified as pixels belonging to fronts). Then we computed the median of Chl-a over these frontal pixels. Note that our quantification depends on the data availability.

We also computed the local excess of Chl-a, E , express in percent, defined as the median value over fronts minus the median value of total Chl-a, divided by the median value of total Chl-a:

$$195 \quad E = \frac{Chl_{front} - Chl_{tot}}{Chl_{tot}} \quad (1)$$

This metric quantifies the relative enrichment of Chl-a at frontal zones compared to the background.

Haëck et al. (2023) make a difference between weak fronts ($5 < HI < 10$) and strong fronts ($HI > 10$) since Chl-a increased with front intensity. In our study, we also started by distinguishing two groups of front according to their intensity. Nevertheless, when we analyzed the distribution of Chl-a over the different groups, Chl-a over weak fronts were close to Chl-a outside
200 fronts ($5 < HI$). This aligned with the results of Tzortzis et al. (2021), which showed that moderate energetic fronts in the



Mediterranean Sea are mostly dynamical barriers between phytoplankton communities. Thus, we focused exclusively on strong fronts for both HI and FSLE analysis.

To evaluate the statistical significance of Chl-a differences over and outside frontal regions, we computed the probability density functions of Chl-a over and outside fronts, from 1998 to 2021 and from 2016 to 2021. From these distributions, we randomly selected 300 samples from each pool and compared them with the Brunner-Munzel statistical test. This nonparametric test assessed the null hypothesis that, for random samples X and Y from two distributions, the probability of X being higher than Y is equal to the probability of X being lower than Y. We selected the Brunner-Munzel test due to its robustness in scenarios where distributions showed unequal variances, unlike the Mann-Whitney U test. This comparison was conducted regionally and seasonally across 23 years of data.

We also investigated the local impact of fronts on phytoplankton community structure. For each day, we calculated the mean proportion of each pigment-derived phytoplankton groups over and outside fronts. We then computed the anomaly for each phytoplankton groups to highlight their response to fronts. This analysis is performed for each region and over the 23-years and 6-years periods, allowing us to characterize the mean seasonal variability in phytoplankton groups proportions associated with frontal presence.

3 Results

3.1 Characterization of fine scale fronts distribution

We start by characterizing the distribution of fronts detected by SST, density and FSLE data, by computing the occurrence (Figure 2).

Our results reveal a similar distribution between fronts detected by SST and density but pronounced disparities with the distribution of fronts detected by FSLE, consistent with Sudre et al. (2023b). Fronts with SST outline persistent oceanographic structures, including the Alboran Gyre, the Liguro-Provençal Current within the Gulf of Lion, and the Rhodes and Ierapetra gyres in the Levantine region (Figure 2a). Fronts identified by density highlight the same structures but with higher occurrence values (Figure 2c). Fronts derived both from AVISO and 4DMED data exhibit a homogeneous distribution across the Alboran region, much of the Algerian-Tyrrhenian basin, and the Ionian-Levantine region, where fronts delineate the boundaries of numerous eddies passing by (Figure 2b). However, marked differences emerge between these two distributions. Occurrences from AVISO-FSLE are weaker throughout the basin and even absent in the smaller regions like the Gulf of Lion. In contrast, fronts from 4DMED-FSLE are characterized by higher occurrences everywhere, even in the Gulf of Lion (Figure 2d). We suggest that because AVISO-FSLE are derived from SSALTO/DUACS geostrophic currents at a resolution of $1/4^\circ$, fronts associated to finer currents might be missed in the Gulf of Lion.

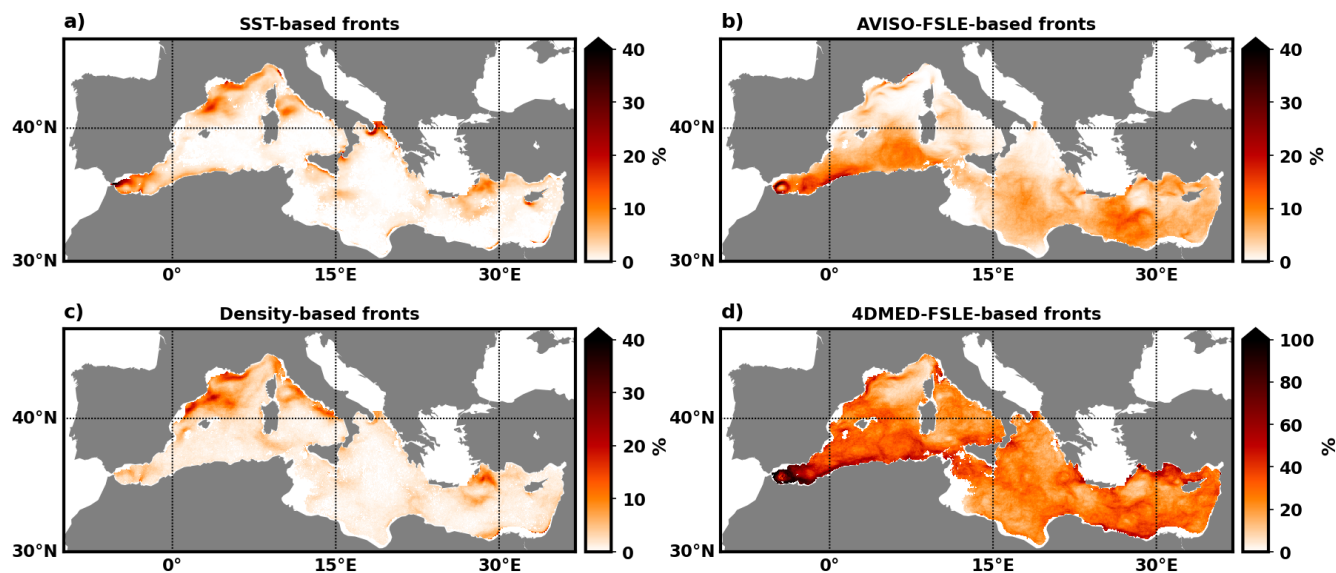


Figure 2. Occurrence of (a) fronts from SST fields and (b) fronts from AVISO-FSLE data over the period 1998-2021, and (c) fronts from density fields and (d) fronts from 4DMED-FSLE data over the period of 2016-2021. The occurrence is expressed as the percentage of time for which a pixel is occupied by a front. Note that the colorbar scale for panel (d) is adjusted to prevent saturation and improve map visibility.

230 3.2 Front effect on phytoplankton biomass

3.2.1 SST-based fronts

We found that fronts detected from SST diagnostics systematically enhance Chl-a, especially in summers low-productivity regimes or in oligotrophic conditions.

In the Alboran basin, a large enhancement in fronts is observable in spring, with a Chl-a average of 0.43 mg.m^{-3} (Figure 235 3a), representing an excess of 35.1% compared to the total Chl-a (Figures 3a, c and 5a). The Chl-a excess remains above 20% for the rest of the year, and falls sharply to 4% in winter. In the Gulf of Lion, fronts have a favorable effect in winter by sustaining a Chl-a excess of 17.8% (not significant in Figure 5), associated to a Chl-a mean of 0.36 mg.m^{-3} . In spring, this excess sharply decreases to 4.6% (Figure 3f and Figure 5a), coinciding with the large-scale spring bloom event (Figure 3d). Summer and autumn are characterized by larger Chl-a excess in fronts of 15% and 13.5%, respectively. In the Algerian- 240 Tyrrhenian and Ionian-Levantine basins, fronts induces similar Chl-a seasonal variability and excess values (Figures 3o and r and Figure 5a). Their influence is larger in summer than in winter, despite lower Chl-a values during summer. For instance, in the Algerian-Tyrrhenian basin, Chl-a are approximately 0.28 mg.m^{-3} in winter and 0.12 mg.m^{-3} in summer. However, the Chl-a excess associated with fronts is less than 10% in winter but reaches 22.2% in summer.

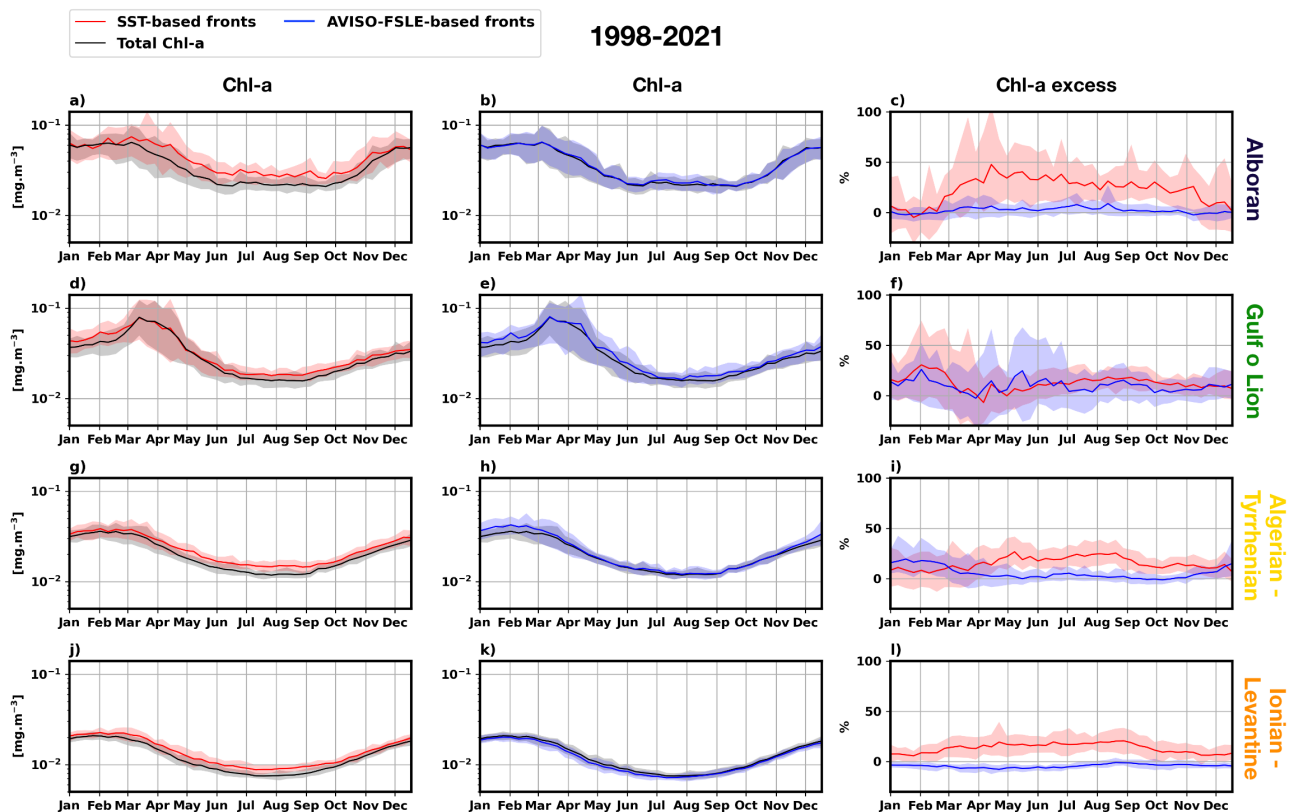


Figure 3. Seasonal variability of Chl-a median values and excess of Chl-a averaged over the period 1998–2021, for each region (per row) described on Figure 1. Total Chl-a are shown in black, values computed over fronts detected from SST fields in red and fronts from AVISO-FLSE data in blue. The plain lines represent the climatological mean of 8-day distributions, and the envelopes mark the 10% and 90% percentile across the entire time series.

3.2.2 Density-based fronts

245 Our analysis of fronts detected from HI over density fields highlights the consistent enhancement of Chl-a at front-scale, still larger in low-productivity conditions, while the front effect is negligible in eutrophic conditions such as the spring bloom event in the Gulf of Lion (Figures 4d and 5c). The seasonal variability of fronts effect still aligns with the regional seasonal variability (Figure 4a, d, g and j). In the Alboran and Ionian-Levantine basins, the effect of fronts is more pronounced in summer, during low-productivity regimes, rather than in winter during the large-scale bloom event (Figures 4a, j and 5c). In contrast, in the

250 Gulf of Lion and Algerian-Tyrrhenian basins, fronts have a stronger influence in winter-autumn than in summer (Figures 4d, g). The larger phytoplankton enhancement remains in the Alboran region in summer, reaching up to 35.6% of Chl-a excess (Figure 5c).



3.2.3 FSLE-based fronts

Fronts detected using FSLE diagnostics do not show a consistent enhancement of phytoplankton biomass (Figures 3b, e, h, k
255 and 4b, e, h, k). Most of the Chl-a excess results are non-significant or negative. We supposed that this likely reflects limitations
in the effective resolution and front localization of FSLE diagnostics, rather than the absence of a biological response to frontal
dynamics.

In the Alboran region, although fronts are prominent features (Figure 2b, d), there is no phytoplankton enrichment related
(Figures 3b, c and 4b, c). Chl-a excess are non-significant with fronts from AVISO-FSLE data, and mostly negative with
260 fronts from 4DMED-FSLE data (Figure 5b, d).

In the Gulf of Lion, fronts sustain a Chl-a enhancement in summer, with an excess from 5.7% to 10.3% (Figures 5b, d),
while this effect disappeared for the rest of the year (Figures 3e, f and 4e, f).

In the Algerian-Tyrrhenian region, fronts from AVISO-FSLE have a positive effect in winter with a Chl-a excess reaching
up to 15.1%, which declines sharply to 2.8% in summer. The Ionian-Levantine region is characterized by negative values of
265 Chl-a excess (Figures 3k, l and 4k, l), ranging from -3% to -6% (Figures 5b, d). In both regions, Chl-a excess associated with
4DMED-FSLE fronts are not statistically significant.

3.3 Shift in phytoplankton community structure

Our previous results indicate that fronts detected from SST and density have a stronger effect on phytoplankton growth, with
Chl-a excess reaching up to 35%, than FSLE-based fronts. To investigate further how this influence shapes phytoplankton
270 composition, we quantify the impact of fronts on phytoplankton community structures using pigment-derived phytoplankton
groups data. Here we present only the analyses for fronts detected from SST and density fields, as results for FSLE-based fronts
were not significant. The seasonal average proportions of phytoplankton groups for each region are presented in Supplemen-
tary Figure A1, revealing a Mediterranean-wide dominance of the other eukaryotes group. Diatoms and prokaryotes seasonally
alternate as the second-most abundant phytoplankton group. In Figures 6 and 7, we present front-scale anomalies of phyto-
275 plankton groups proportions, showing how fronts influence the contribution of a group within the phytoplankton community.
This allows us to investigate whether fronts drive shifts in phytoplankton community composition.

A consistent pattern across the regions is the systematic increase in diatom proportions and the concomitant decrease in
prokaryotes within fronts (Figures 6 and 7). For example, SST-derived fronts induce a large shift in summer in the Alboran
region, with an increase of 3.57% of diatom proportion while the proportion of prokaryotes decreases of -2.88% (Figure 6).
280 When assessing relative changes, meaning the proportional change within each group itself, we find that diatom proportions
increase by 20%, while prokaryote proportions decrease by -13%. This highlights both how fronts reshape community structure
and how they independently enhance or reduce the proportion of each phytoplankton group. Besides, the seasonal variability
of diatoms anomaly mirrors the seasonal cycle of Chl-a excess, reinforcing that diatoms are a key contributor to the Chl-a
enhancement over fronts (Figures 3c, f, i, l and 4c, f, i, l).

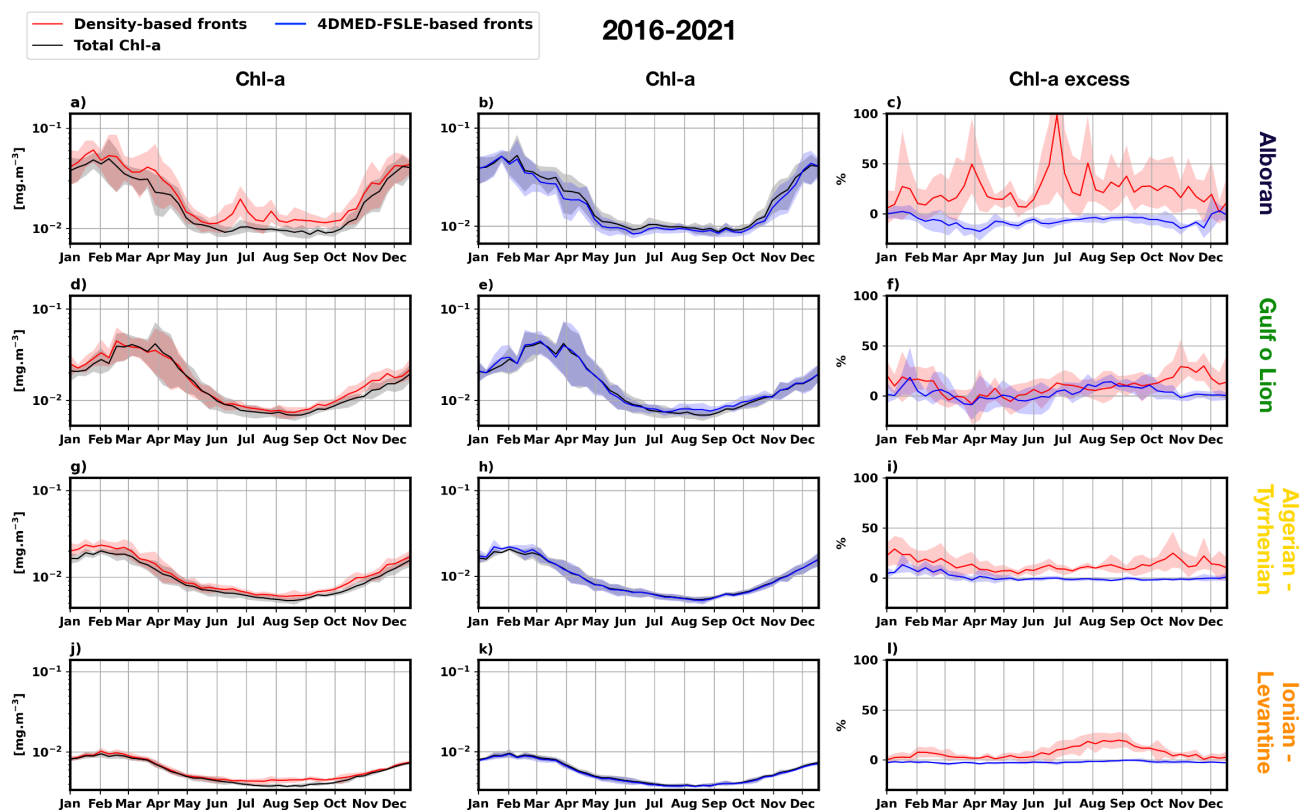


Figure 4. Seasonal variability of Chl-a median values and excess of Chl-a averaged over the period 2016–2021, for each region (per row) described on Figure 1. Total Chl-a are shown in black, values computed over fronts from density fields in red and fronts from 4DMED-FSLE in blue. The plain lines represent the climatological mean of 8-day distributions, and the envelopes mark the 10% and 90% percentile across the entire time series.

285 The response of the other eukaryotes group is not consistent. Relative to the total community, their proportion decreases at front-scale throughout the year in the Alboran Sea. But this response differs in the rest of the Mediterranean Sea and some co-enrichment with diatoms can occur regarding the context. In Algerian-Tyrrhenian and Ionian-Levantine regions, for example, seasonal increases in Chl-a excess over SST-detected fronts (from spring to autumn) coincide with proportional increases in both diatoms and other eukaryotes. A similar co-enrichment pattern occurs in fronts detected from density during spring and
 290 summer in the Algerian-Tyrrhenian basin.

4 Discussion

Our results provide both new insights into phytoplankton-front interactions in the Mediterranean Sea and a comparative assessment of how different detection methods capture these relationships. They highlight the pronounced effect of fronts on



a)	SST-based fronts				b)	AVIS0-FSLE-based fronts			
	Winter	Spring	Summer	Autumn		Winter	Spring	Summer	Autumn
Alboran	3.9±23.3	33.8±32.2	29.9±21.4	21.9±20.9	Alboran	-0.5±6.5	-	-	-
Gulf of Lion	-	4.5±28.0	14.2±11.2	12.2±9.6	Gulf of Lion	-	-	10.3±20.8	-
Alg-Tyr	9.0±13.0	16.6±14.1	21.8±9.7	13.0±7.4	Alg-Tyr	15.1±13.1	-	2.8±5.7	-
Ion-Lev	8.2±7.8	15.8±9.6	18.3±8.9	-	Ion-Lev	-3.8±3.1	-6.4±3.3	-3.9±3.3	-
c)	Density-based fronts				d)	4DMED-FSLE-based fronts			
	Winter	Spring	Summer	Autumn		Winter	Spring	Summer	Autumn
Alboran	13.4±23.0	19.9±22.3	35.6±41.2	23.9±21.2	Alboran	-1.7±-1.7	-	-6.2±-6.2	-8.1±-8.1
Gulf of Lion	13.9±15.7	-1.1±12.4	8.1±10.8	18.4±14.0	Gulf of Lion	-	-	5.7±5.7	-
Alg-Tyr	18.6±12.2	9.1±7.8	10.2±4.9	15.0±11.7	Alg-Tyr	-	-0.2±-0.2	-	-
Ion-Lev	3.8±4.8	-	13.1±8.7	8.5±7.0	Ion-Lev	-	-3.0±-3.0	-	-

Figure 5. Table of average seasonal of Chl-a excess values with the standard deviation sustained by fronts from SST fields (a), fronts from AVIS0-FSLE fields (b), fronts from density fields (c) and fronts from 4DMED-FSLE fields (d) for each region. Positive values are shown in green and negative values in pink. Excess values are shown when the differences between distributions within and outside the fronts are statistically significant.

both phytoplankton biomass and community structure, with the strongest effects observed during low-productivity regimes. However, the observed ecological responses vary to the choice of front detection method used.

Local enhancements of Chl-a at fronts detected from SST and density diagnostics are systematic, by 4% to 35%, with stronger effects in oligotrophic regions and during stratified periods. Our findings aligns with those of Liu and Levine (2016) which found a local increase of 38% in fronts detected from SST within the North Pacific subtropical gyre, and Haëck et al. (2023) which measured an increase of more than 60% at front scale in the vicinity of the the Gulf Stream. This result is consistent with the fact that strong density gradients are associated with ageostrophic secondary circulation and vertical nutrient fluxes, which are key mechanisms controlling phytoplankton growth at fronts.



1998-2021

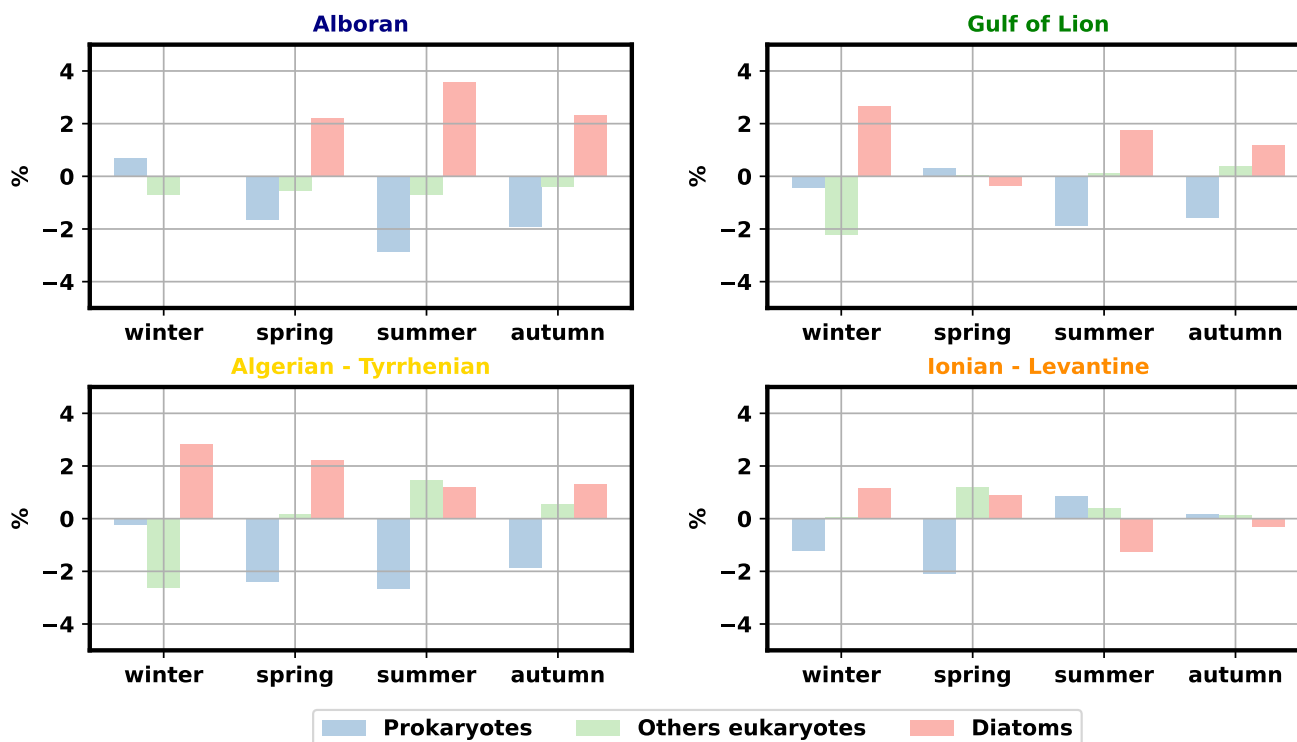


Figure 6. Anomaly of phytoplankton community composition over fronts detected from SST fields within each bioregion. The averages are computed over the full period 1998-2021. Diatoms are in red, other eukaryotes in green and prokaryotes in blue.

In contrast, fronts detected using FSLE diagnostics show a weaker relationship with changes in phytoplankton biomass. This result is likely due to a limitation of the FSLE diagnostic in resolving and localizing fronts accurately enough to co-localize them with the fine-scale biological signal seen in satellite ocean color data. Because FSLE fields are derived from altimetric currents, their effective spatial resolution may not be sufficient to capture the exact localization of fronts associated to finer currents that drive vertical exchanges. The differences observed between HI and FSLE diagnostics suggest that the detection method is key in evaluating the magnitude of the observed phytoplankton response. Our results raise questions about the suitability of FSLE data for studying the impact of density-driven vertical exchanges at fronts on phytoplankton at the scale of fronts. The results from the Gulf of Lion region are surprising: while we expected the phytoplankton-front interaction to be influenced by the improved representation of fronts from the 4DMED-FSLE data, this was not the case. Minor discrepancies between the two analyses can be attributed to differences in their respective study periods and the higher spatial resolution of the 4DMED-FSLE dataset.

Beyond methodological aspects, our results provide new insights into the spatial and seasonal variability of phytoplankton responses to fronts in the Mediterranean Sea. The stronger response observed in oligotrophic regions and during summer



2016-2021

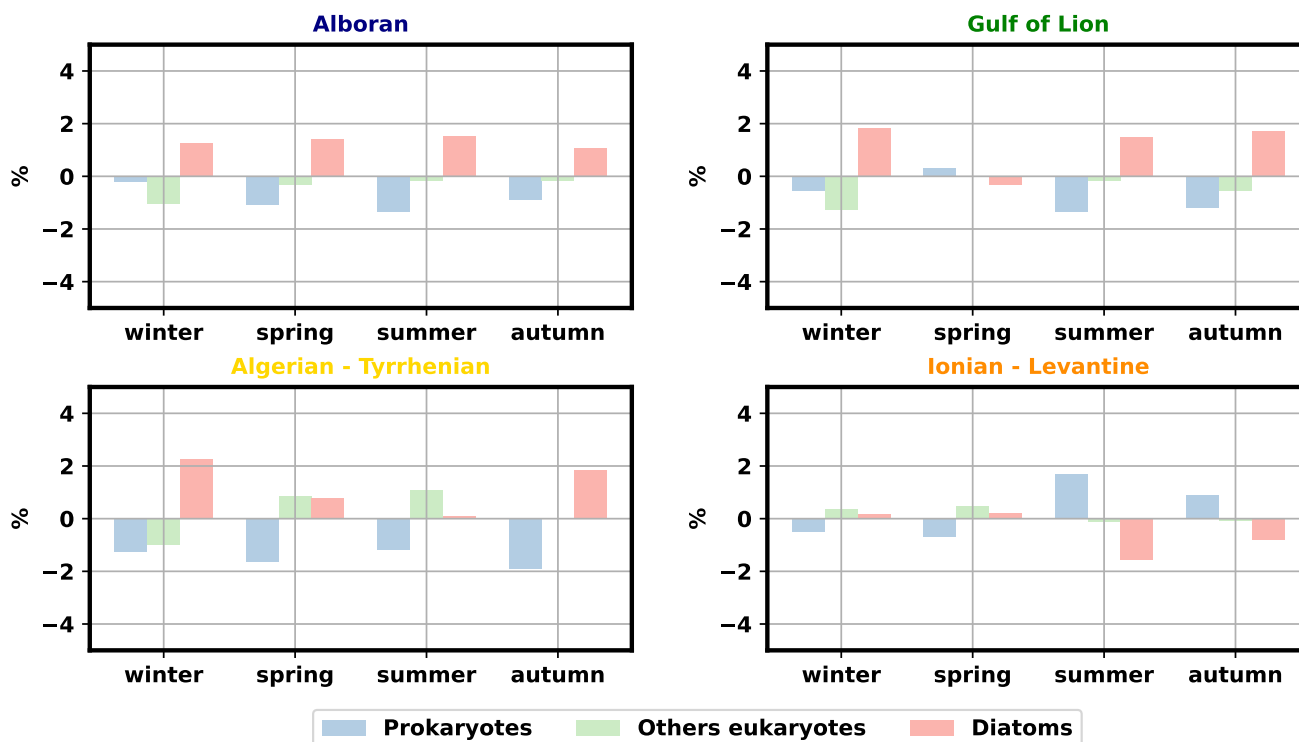


Figure 7. Excess of phytoplankton community composition over fronts detected from density fields within each bioregions. The averages are computed over the full period 2016-2021. Diatoms are in red, other eukaryotes in green and prokaryotes in blue.

315 suggests that fronts play a particularly important role in nutrient-limited environments. During summer, enhanced vertical stratification leads to the formation of a shallow mixed layer, promoting oligotrophic conditions and reduced surface Chl-a. In such oligotrophic environments where phytoplankton growth is nutrient-limited, frontal processes can sustain localized nutrient supply through vertical transport (Mahadevan, 2016; Lévy et al., 2018) or horizontal stirring (Fadida et al., 2026). This influence is weaker during winter and spring, when deepening of the mixed layer supplies nutrients that drive large-scale
 320 bloom. Although fronts may still enhance local nutrient fluxes to the surface, it does not influence phytoplankton growth due to the basin-wide contribution of mixed-layer deepening. We suggest that regional differences may also arise from regional variations in stratification structure, nutricline depth, or the efficiency of vertical velocities in reaching the nutricline.

The observed shifts in phytoplankton community composition, including diatom enrichment and prokaryotes depletion at fronts, further support the role of frontal processes in structuring marine ecosystems in this region. Our findings reveal a consistent increase of diatoms at frontal scales, up to 20%, whenever phytoplankton biomass is enhanced over fronts. These results
 325 are consistent with previous studies showing that frontal dynamics can enhance nutrient supply and favor larger phytoplank-



ton, related to their adaptability to the rapidly changing conditions (Lévy et al., 2015; Liu and Levine, 2021; Mangolte et al., 2022, 2023; Lévy et al., 2025), while reducing the relative contribution of smaller oligotrophic-adapted organisms.

Our results also reveal a complex response within the other eukaryotes group, which occasionally benefits from frontal dynamics, especially in the two larger basins. Unlike the diatom-specific enrichment observed in the Alboran region, our results suggest that both diatoms and other eukaryotes groups benefit from frontal conditions (Figures 6 and 7). In certain cases, fronts are not associated with a single, uniform plankton community, rather some plankton types may be more or less favored, or even disadvantaged, depending on the specific environmental context (e.g., d'Ovidio et al., 2004; Tzortzis et al., 2021; Mangolte et al., 2022, 2023). While nutrient inputs at fronts primarily drive the dominance of fast-growing species, other processes can also play a large role in phytoplankton diversity such as abiotic processes (horizontal advection, Gangrade and Franks, 2023) and reactive processes (light competition, shared predation pressure, Lévy et al., 2018; Mangolte et al., 2022). In the western Mediterranean Sea, Oms et al. (2024) used an NPZ model to explain the coexistence of picophytoplankton and microphytoplankton groups near fine-scale fronts observed by Tzortzis et al. (2021). Their analysis show that pulsed nutrient inputs affect the system by combining bottom-up and top-down controls through zooplankton, leading to complex seascape of phytoplankton communities.

Several limitations should be considered when interpreting our results. Differences in spatial resolution, temporal coverage, and physical meaning between diagnostics may affect the comparison. In particular, FSLE diagnostics may fail at precisely locating fronts, while SST may fail to capture density-compensated fronts. Indeed, the comparison between SST and density fronts (occurrence, distribution and Chl-a excess) also highlights the role of thermohaline compensation, which can lead to strong temperature gradients without significant density gradients and therefore without enhanced vertical exchanges. It reinforces the idea that fronts detected from density fields provide a direct representation of the physical structure of fronts and show consistent biological responses, supporting the central role of density gradients in controlling phytoplankton dynamics. Finally, phytoplankton responses to frontal dynamics may not be instantaneous (Gangrade and Franks, 2023; Gangrade and Mangolte, 2024), and therefore the systematic co-localisation of fronts and of their biological response, as assumed here and in previous studies (e.g., Haëck et al., 2023; Lévy et al., 2025), may underestimate the impact of fronts when the biological signal is advected away from the front.

Overall, our results demonstrate that the quantification of the apparent ecological impact of fronts depends strongly on both the detection method and the nature of the underlying dataset. While the enhancement of phytoplankton biomass at fronts detected from SST and density appears robust, the weaker signal observed for FSLE highlights the importance of carefully selecting diagnostics when studying front–biogeochemistry interactions.

5 Conclusions

This study provides a comprehensive assessment of phytoplankton responses to oceanic fronts across the Mediterranean Sea, combining long-term satellite observations with high-resolution fields reconstructed using in-situ data. Our results show that fronts consistently enhance phytoplankton biomass and influence community composition, with stronger effects in oligotrophic

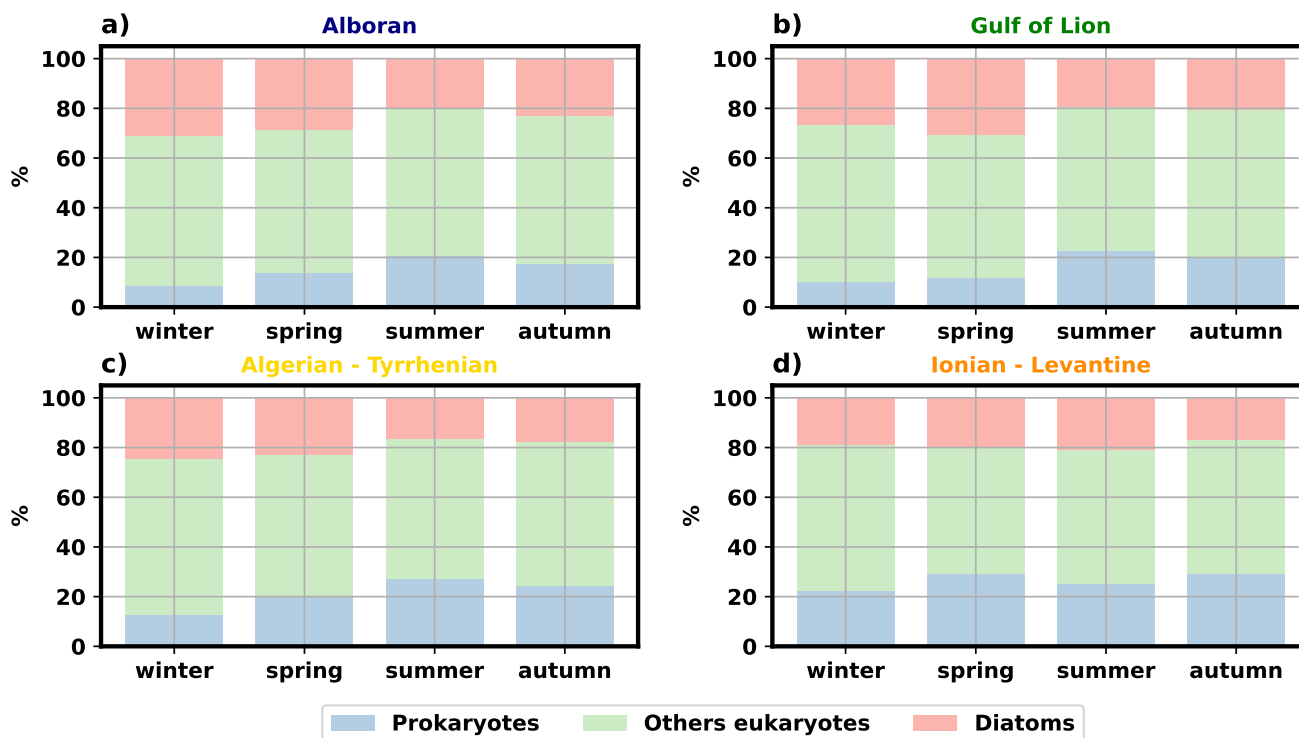


Figure A1. Seasonal time-mean of phytoplankton community composition for each region.

360 regions and during stratified periods. These findings highlight the important role of fronts in structuring marine ecosystems in
 365 nutrient-limited environments such as the Mediterranean Sea. By computing the sensitivity of our results to the front detection
 method and data sets used, we found that SST heterogeneity is the synoptic diagnostics most capable of capturing the spatio-
 temporal scale of an associated biological response.

More broadly, by highlighting the crucial role of fronts in shaping phytoplankton biomass and phenology, our study sus-
 365 tains the idea that changes in oceanic fronts should be considered when investigating ecological reorganization under future
 climate change. Studies evidence undergoing shifts in front intensity and frequency under climate change with profound re-
 gional variability (Xing et al., 2024). While Yang et al. (2023) began documenting trends in fronts and Chl-a, they noted that,
 despite significant trends in ocean warming hotspots, some regions, such as the Mediterranean Sea, do not exhibit statistically
 significant changes. This underscores the need for longer time series to achieve conclusive insights.



370 Appendix A

Data availability. Chl-a GlobColour data were downloaded from the E.U. Copernicus Marine Service (<https://doi.org/10.48670/moi-00280>, Garnesson et al., 2019)). These data have been developed, validated, and distributed by ACRI ST, France. SST data were also downloaded from the E.U. Copernicus Marine Service (<https://doi.org/10.48670/moi-00169>, Good et al., 2020). Surface density fields from the 4DMED-SEA project (Sammartino et al., 2022, 2025) data are available from this repository: <https://opensciencedata.esa.int/products/4dmed-t-s-geo-a-150/collection>. FSLE data from AVISO were downloaded from the AVISO service (10.24400/527896/a01-2022.002, d'Ovidio et al., 2004). The altimeter products were produced by Ssalto/Duacs in collaboration with LOCEAN and CTOH and distributed by Aviso+, with support from CNES (<https://www.aviso.altimetry.fr/>). The FSLE data from 4DMED-SEA project were downloaded from Zenodo repository (<https://zenodo.org/records/11610512>, Cortés-Morales and Hernández-Carrasco, 2024).

Acknowledgements. This research has been part of the project 4DMED-Sea funded by the European Space Agency (ESA). We thank all the members of the 4DMED-Sea project for the useful discussions which helped to improve our analysis and results.

Author contributions. Angelina Cassianides : Conceptualization, Methodology, Data Curation, Visualization, Investigation, Formal analysis, Writing – original draft, Writing – review & editing. Marina Levy : Supervision, Conceptualization, Funding acquisition, Methodology, Investigation, Formal analysis, Writing – original draft, Writing – review & editing. Clément Haëck : Conceptualization, Methodology, Investigation, Writing – review & editing. Ines Mangolte : Formal analysis, Writing – review & editing. Roy El Hourany : Data Curation, Writing – review & editing. Michel Sammartino : Data Curation, Writing – review & editing. Bruno Buongiorno Nardelli : Funding acquisition, Data Curation, Writing – review & editing

Competing interests. The contact author has declared that none of the authors has any competing interests.

Acknowledgements. This research has been part of the project 4DMED-Sea funded by the European Space Agency (ESA). We thank all the members of the 4DMED-Sea project for the useful discussions which helped to improve our analysis and results.



390 References

- Akpınar, A.: Seasonal and Interannual Variability in Sea Surface Temperature Fronts in the Levantine Basin, Mediterranean Sea, *Journal of Marine Science and Engineering*, 12, 1249, <https://doi.org/10.3390/jmse12081249>, 2024.
- Barral, Q.-B., Zakardjian, B., Dumas, F., Garreau, P., Testor, P., and Beuvier, J.: Characterization of fronts in the Western Mediterranean with a special focus on the North Balearic Front, *Progress in Oceanography*, 197, 102 636, <https://doi.org/10.1016/j.pocean.2021.102636>,
395 2021.
- Baudena, A., Ser-Giacomi, E., D’Onofrio, D., Capet, X., Cotté, C., Cherel, Y., and D’Ovidio, F.: Fine-scale structures as spots of increased fish concentration in the open ocean, *Scientific Reports*, 11, 15 805, <https://doi.org/10.1038/s41598-021-94368-1>, 2021.
- Belkin, I. M. and O’Reilly, J. E.: An algorithm for oceanic front detection in chlorophyll and SST satellite imagery, *Journal of Marine Systems*, 78, 319–326, <https://doi.org/10.1016/j.jmarsys.2008.11.018>, 2009.
- 400 Bost, C., Cotté, C., Bailleul, F., Cherel, Y., Charrassin, J., Guinet, C., Ainley, D., and Weimerskirch, H.: The importance of oceanographic fronts to marine birds and mammals of the southern oceans, *Journal of Marine Systems*, 78, 363–376, <https://doi.org/10.1016/j.jmarsys.2008.11.022>, 2009.
- Capó, E., Orfila, A., Mason, E., and Ruiz, S.: Energy Conversion Routes in the Western Mediterranean Sea Estimated from Eddy–Mean Flow Interactions, *Journal of Physical Oceanography*, 49, 247–267, <https://doi.org/10.1175/JPO-D-18-0036.1>, 2019.
- 405 Cayula, J.-F. and Cornillon, P.: Edge Detection Algorithm for SST Images, *Journal of Atmospheric and Oceanic Technology*, 9, 67–80, [https://doi.org/10.1175/1520-0426\(1992\)009<0067:EDAFSI>2.0.CO;2](https://doi.org/10.1175/1520-0426(1992)009<0067:EDAFSI>2.0.CO;2), 1992.
- Cortés-Morales, D. and Hernández-Carrasco, I.: ESA 4DMED-Sea - Finite-size Lyapunov Exponents in the Mediterranean Sea derived from 4DVARNET8 geostrophic velocities ($1/24^\circ$), <https://doi.org/https://doi.org/10.5281/zenodo.11612964>, 2024.
- d’Ovidio, F., Fernández, V., Hernández-García, E., and López, C.: Mixing structures in the Mediterranean Sea from finite-size Lyapunov
410 exponents, *Geophysical Research Letters*, 31, <https://doi.org/10.1029/2004GL020328>, 2004.
- D’Asaro, E., Lee, C., Rainville, L., Harcourt, R., and Thomas, L.: Enhanced Turbulence and Energy Dissipation at Ocean Fronts, *Science*, 332, 318–322, <https://doi.org/10.1126/science.1201515>, 2011.
- Fablet, R., Beauchamp, M., Drumetz, L., and Rousseau, F.: Joint Interpolation and Representation Learning for Irregularly Sampled Satellite-Derived Geophysical Fields, *Frontiers in Applied Mathematics and Statistics*, 7, <https://doi.org/10.3389/fams.2021.655224>, 2021.
- 415 Fadida, Y., Verma, V., Barkan, R., Biton, E., Solodoch, A., and Lehahn, Y.: Coastal-to-offshore submesoscale horizontal stirring enhances wintertime phytoplankton blooms in the ultra-oligotrophic Eastern Mediterranean Sea, *Ocean Science*, 22, 329–343, <https://doi.org/10.5194/os-22-329-2026>, 2026.
- Fox-Kemper, B., Ferrari, R., and Hallberg, R.: Parameterization of Mixed Layer Eddies. Part I: Theory and Diagnosis, *Journal of Physical Oceanography*, 38, 1145–1165, <https://doi.org/10.1175/2007JPO3792.1>, 2008.
- 420 Gangrade, S. and Franks, P. J. S.: Phytoplankton Patches at Oceanic Fronts Are Linked to Coastal Upwelling Pulses: Observations and Implications in the California Current System, *Journal of Geophysical Research: Oceans*, 128, <https://doi.org/10.1029/2022JC019095>, 2023.
- Gangrade, S. and Mangolte, I.: Patchiness of plankton communities at fronts explained by Lagrangian history of upwelled water parcels, *Limnology and Oceanography*, 69, 2123–2137, <https://doi.org/10.1002/lno.12654>, 2024.



- 425 García-Olivares, A., Isern-Fontanet, J., and García-Ladona, E.: Dispersion of passive tracers and finite-scale Lyapunov exponents in the Western Mediterranean Sea, *Deep Sea Research Part I: Oceanographic Research Papers*, 54, 253–268, <https://doi.org/10.1016/j.dsr.2006.10.009>, 2007.
- Garnesson, P., Mangin, A., and Bretagnon, M.: Quality User Guide, Ocean Colour Production Centre, Satellite Observation GlobColour-Copernicus Products, <https://doi.org/https://doi.org/10.48670/moi-00280>, 2019.
- 430 Good, S., Fiedler, E., Mao, C., Martin, M. J., Maycock, A., Reid, R., Roberts-Jones, J., Searle, T., Waters, J., While, J., and Worsfold, M.: The Current Configuration of the OSTIA System for Operational Production of Foundation Sea Surface Temperature and Ice Concentration Analyses, *Remote Sensing*, 12, 720, <https://doi.org/10.3390/rs12040720>, 2020.
- Haëck, C., Lévy, M., Mangolte, I., and Bopp, L.: Satellite data reveal earlier and stronger phytoplankton blooms over fronts in the Gulf Stream region, *Biogeosciences*, 20, 1741–1758, <https://doi.org/10.5194/bg-20-1741-2023>, 2023.
- 435 Heimbürger, L.-E., Lavigne, H., Migon, C., D’Ortenzio, F., Estournel, C., Coppola, L., and Miquel, J.-C.: Temporal variability of vertical export flux at the DYFAMED time-series station (Northwestern Mediterranean Sea), *Progress in Oceanography*, 119, 59–67, <https://doi.org/10.1016/j.pocean.2013.08.005>, 2013.
- Hernández-Carrasco, I., López, C., Hernández-García, E., and Turiel, A.: How reliable are finite-size Lyapunov exponents for the assessment of ocean dynamics?, *Ocean Modelling*, 36, 208–218, <https://doi.org/10.1016/j.ocemod.2010.12.006>, 2011.
- 440 Hernández-Carrasco, I., Alou-Font, E., Dumont, P.-A., Cabornero, A., Allen, J., and Orfila, A.: Lagrangian flow effects on phytoplankton abundance and composition along filament-like structures, *Progress in Oceanography*, 189, 102469, <https://doi.org/10.1016/j.pocean.2020.102469>, 2020.
- Hernández-Carrasco, I. and Orfila, A.: The Role of an Intense Front on the Connectivity of the Western Mediterranean Sea: The Cartagena-Tenes Front, *Journal of Geophysical Research: Oceans*, 123, 4398–4422, <https://doi.org/10.1029/2017JC013613>, 2018.
- 445 Hourany, R. E., Saab, M. A., Faour, G., Aumont, O., Crépon, M., and Thiria, S.: Estimation of Secondary Phytoplankton Pigments From Satellite Observations Using Self-Organizing Maps (SOMs), *Journal of Geophysical Research: Oceans*, 124, 1357–1378, <https://doi.org/10.1029/2018JC014450>, 2019.
- Hourany, R. E., Mejia, C., Faour, G., Crépon, M., and Thiria, S.: Evidencing the Impact of Climate Change on the Phytoplankton Community of the Mediterranean Sea Through a Bioregionalization Approach, *Journal of Geophysical Research: Oceans*, 126, <https://doi.org/10.1029/2020JC016808>, 2021.
- 450 Lazzari, P., Solidoro, C., Ibello, V., Salon, S., Teruzzi, A., Béranger, K., Colella, S., and Crise, A.: Seasonal and inter-annual variability of plankton chlorophyll and primary production in the Mediterranean Sea: a modelling approach, <https://doi.org/10.5194/bgd-8-5379-2011>, 2011.
- Lehahn, Y., d’Ovidio, F., Lévy, M., and Heifetz, E.: Stirring of the northeast Atlantic spring bloom: A Lagrangian analysis based on multi-satellite data, *Journal of Geophysical Research: Oceans*, 112, <https://doi.org/10.1029/2006JC003927>, 2007.
- 455 Li, Y., Liang, J., Da, H., Chang, L., and Li, H.: A Deep Learning Method for Ocean Front Extraction in Remote Sensing Imagery, *IEEE Geoscience and Remote Sensing Letters*, 19, 1–5, <https://doi.org/10.1109/LGRS.2021.3081179>, 2022.
- Liu, X. and Levine, N. M.: Enhancement of phytoplankton chlorophyll by submesoscale frontal dynamics in the North Pacific Subtropical Gyre, *Geophysical Research Letters*, 43, 1651–1659, <https://doi.org/10.1002/2015GL066996>, 2016.
- 460 Liu, X. and Levine, N. M.: Ecosystem implications of fine-scale frontal disturbances in the oligotrophic ocean – An idealized modeling approach, *Progress in Oceanography*, 192, 102519, <https://doi.org/10.1016/j.pocean.2021.102519>, 2021.



- Lévy, M., Mémerly, L., and Madec, G.: The onset of a bloom after deep winter convection in the northwestern Mediterranean sea: mesoscale process study with a primitive equation model, *Journal of Marine Systems*, 16, 7–21, [https://doi.org/10.1016/S0924-7963\(97\)00097-3](https://doi.org/10.1016/S0924-7963(97)00097-3), 1998.
- 465 Lévy, M., Jahn, O., Dutkiewicz, S., Follows, M. J., and d’Ovidio, F.: The dynamical landscape of marine phytoplankton diversity, *Journal of The Royal Society Interface*, 12, 20150481, <https://doi.org/10.1098/rsif.2015.0481>, 2015.
- Lévy, M., Franks, P. J. S., and Smith, K. S.: The role of submesoscale currents in structuring marine ecosystems, *Nature Communications*, 9, 4758, <https://doi.org/10.1038/s41467-018-07059-3>, 2018.
- Lévy, M., Haëck, C., Mangolte, I., Cassianides, A., and Hourany, R. E.: Shift in phytoplankton community composition over fronts, *Communications Earth & Environment*, 6, 591, <https://doi.org/10.1038/s43247-025-02553-1>, 2025.
- 470 Macías, D., Bruno, M., Echevarría, F., Vázquez, A., and García, C.: Meteorologically-induced mesoscale variability of the North-western Alboran Sea (southern Spain) and related biological patterns, *Estuarine, Coastal and Shelf Science*, 78, 250–266, <https://doi.org/10.1016/j.ecss.2007.12.008>, 2008.
- Mahadevan, A.: The Impact of Submesoscale Physics on Primary Productivity of Plankton, *Annual Review of Marine Science*, 8, 161–184, <https://doi.org/10.1146/annurev-marine-010814-015912>, 2016.
- 475 Mangolte, I., Lévy, M., Dutkiewicz, S., Clayton, S., and Jahn, O.: Plankton community response to fronts: winners and losers, *Journal of Plankton Research*, 44, 241–258, <https://doi.org/10.1093/plankt/fbac010>, 2022.
- Mangolte, I., Lévy, M., Haëck, C., and Ohman, M. D.: Sub-frontal niches of plankton communities driven by transport and trophic interactions at ocean fronts, *Biogeosciences*, 20, 3273–3299, <https://doi.org/10.5194/bg-20-3273-2023>, 2023.
- 480 Mauzole, Y. L., Torres, H. S., and Fu, L.: Patterns and Dynamics of SST Fronts in the California Current System, *Journal of Geophysical Research: Oceans*, 125, <https://doi.org/10.1029/2019JC015499>, 2020.
- Mayot, N., D’Ortenzio, F., Taillandier, V., Prieur, L., de Fommervault, O. P., Claustre, H., Bosse, A., Testor, P., and Conan, P.: Physical and Biogeochemical Controls of the Phytoplankton Blooms in North Western Mediterranean Sea: A Multiplatform Approach Over a Complete Annual Cycle (2012–2013 DEWEX Experiment), *Journal of Geophysical Research: Oceans*, 122, 9999–10019, <https://doi.org/10.1002/2016JC012052>, 2017.
- 485 McKee, D. C., Doney, S. C., Penna, A. D., Boss, E. S., Gaube, P., and Behrenfeld, M. J.: Biophysical Dynamics at Ocean Fronts Revealed by Bio-Argo Floats, *Journal of Geophysical Research: Oceans*, 128, <https://doi.org/10.1029/2022JC019226>, 2023.
- Mercado, J. M., Cortés, D., Ramírez, T., and Gómez, F.: Decadal weakening of the wind-induced upwelling reduces the impact of nutrient pollution in the Bay of Málaga (western Mediterranean Sea), *Hydrobiologia*, 680, 91–107, <https://doi.org/10.1007/s10750-011-0906-y>, 2012.
- 490 Merchant, C. J., Embury, O., Bulgin, C. E., Block, T., Corlett, G. K., Fiedler, E., Good, S. A., Mittaz, J., Rayner, N. A., Berry, D., Eastwood, S., Taylor, M., Tsushima, Y., Waterfall, A., Wilson, R., and Donlon, C.: Satellite-based time-series of sea-surface temperature since 1981 for climate applications, *Scientific Data*, 6, 223, <https://doi.org/10.1038/s41597-019-0236-x>, 2019.
- Millot, C.: Mesoscale and seasonal variabilities of the circulation in the western Mediterranean, *Dynamics of Atmospheres and Oceans*, 15, 179–214, [https://doi.org/10.1016/0377-0265\(91\)90020-G](https://doi.org/10.1016/0377-0265(91)90020-G), 1991.
- 495 Olita, A., Sparnocchia, S., Cusí, S., Fazioli, L., Sorgente, R., Tintoré, J., and Ribotti, A.: Observations of a phytoplankton spring bloom onset triggered by a density front in NW Mediterranean, *Ocean Science*, 10, 657–666, <https://doi.org/10.5194/os-10-657-2014>, 2014.
- Oms, L., Messié, M., Poggiale, J.-C., Grégori, G., and Doglioli, A.: Fine-scale phytoplankton community transitions in the oligotrophic ocean: A Mediterranean Sea case study, *Journal of Marine Systems*, 246, 104021, <https://doi.org/10.1016/j.jmarsys.2024.104021>, 2024.



- 500 Oms, L., Doglioli, A., Messié, M., d'Ovidio, F., Capet, X., Rousselet, L., Joel, A., Izard, L., Lévy, M., Berta, M., Petrenko, A., Bellacicco, M., Barrillon, S., Grand, L., Pulido-Villena, E., Nunige, S., Leblanc, K., Courtois, B., Zhang, W., and Grégori, G.: Fine-scale observations reveal distinct frontal phytoplankton communities, *Communications Earth & Environment*, 7, 468, <https://doi.org/10.1038/s43247-026-03350-0>, 2026.
- Pegliasco, C., Chaigneau, A., Morrow, R., and Dumas, F.: Detection and tracking of mesoscale eddies in the Mediterranean Sea: A comparison between the Sea Level Anomaly and the Absolute Dynamic Topography fields, *Advances in Space Research*, 68, 401–419, <https://doi.org/10.1016/j.asr.2020.03.039>, 2021.
- Renault, L., Oguz, T., Pascual, A., Vizoso, G., and Tintore, J.: Surface circulation in the Alborán Sea (western Mediterranean) inferred from remotely sensed data, *Journal of Geophysical Research: Oceans*, 117, <https://doi.org/10.1029/2011JC007659>, 2012.
- Ruiz, S., Claret, M., Pascual, A., Olita, A., Troupin, C., Capet, A., Tovar-Sánchez, A., Allen, J., Poulain, P., Tintoré, J., and Mahadevan, A.: Effects of Oceanic Mesoscale and Submesoscale Frontal Processes on the Vertical Transport of Phytoplankton, *Journal of Geophysical Research: Oceans*, 124, 5999–6014, <https://doi.org/10.1029/2019JC015034>, 2019.
- 510 Sala, I., Bolado-Penagos, M., Bartual, A., Bruno, M., García, C. M., Ángel López-Urrutia, González-García, C., and Echevarría, F.: A Lagrangian approach to the Atlantic Jet entering the Mediterranean Sea: Physical and biogeochemical characterization, *Journal of Marine Systems*, 226, 103 652, <https://doi.org/10.1016/j.jmarsys.2021.103652>, 2022.
- 515 Sammartino, M., Aronica, S., Santoleri, R., and Nardelli, B. B.: Retrieving Mediterranean Sea Surface Salinity Distribution and Interannual Trends from Multi-Sensor Satellite and In Situ Data, *Remote Sensing*, 14, 2502, <https://doi.org/10.3390/rs14102502>, 2022.
- Sammartino, M., Cioppa, L. D., Colella, S., and Nardelli, B. B.: A Physics-informed deep neural network for the joint prediction of 3D chlorophyll-a and hydrographic fields in the Mediterranean Sea, *Environmental Modelling & Software*, 194, 106 660, <https://doi.org/https://doi.org/10.1016/j.envsoft.2025.106660>, 2025.
- 520 Severin, T., Kessouri, F., Rembauville, M., Sánchez-Pérez, E. D., Oriol, L., Caparros, J., Pujo-Pay, M., Ghiglione, J., D'Ortenzio, F., Tailandier, V., Mayot, N., Madron, X. D. D., Ulses, C., Estournel, C., and Conan, P.: Open-ocean convection process: A driver of the winter nutrient supply and the spring phytoplankton distribution in the <sc>N</sc> orthwestern <sc>M</sc> editerranean <sc>S</sc> ea, *Journal of Geophysical Research: Oceans*, 122, 4587–4601, <https://doi.org/10.1002/2016JC012664>, 2017.
- Siegelman, L., O'Toole, M., Flexas, M., Rivière, P., and Klein, P.: Submesoscale ocean fronts act as biological hotspot for southern elephant seal, *Scientific Reports*, 9, 5588, <https://doi.org/10.1038/s41598-019-42117-w>, 2019.
- 525 Siegelman, L., Klein, P., Thompson, A. F., Torres, H. S., and Menemenlis, D.: Altimetry-Based Diagnosis of Deep-Reaching Sub-Mesoscale Ocean Fronts, *Fluids*, 5, 145, <https://doi.org/10.3390/fluids5030145>, 2020.
- Siokou-Frangou, I., Christaki, U., Mazzocchi, M. G., Montresor, M., d'Alcalá, M. R., Vaqué, D., and Zingone, A.: Plankton in the open Mediterranean Sea: a review, *Biogeosciences*, 7, 1543–1586, <https://doi.org/10.5194/bg-7-1543-2010>, 2010.
- 530 Sudre, F., Dewitte, B., Mazoyer, C., Garçon, V., Sudre, J., Penven, P., and Rossi, V.: Spatial and seasonal variability of horizontal temperature fronts in the Mozambique Channel for both epipelagic and mesopelagic realms, *Frontiers in Marine Science*, 9, <https://doi.org/10.3389/fmars.2022.1045136>, 2023a.
- Sudre, F., Hernández-Carrasco, I., Mazoyer, C., Sudre, J., Dewitte, B., Garçon, V., and Rossi, V.: An ocean front dataset for the Mediterranean sea and southwest Indian ocean, *Scientific Data*, 10, 730, <https://doi.org/10.1038/s41597-023-02615-z>, 2023b.
- 535 Thomas, L. N., Taylor, J. R., D'Asaro, E. A., Lee, C. M., Klymak, J. M., and Shcherbina, A.: Symmetric Instability, Inertial Oscillations, and Turbulence at the Gulf Stream Front, *Journal of Physical Oceanography*, 46, 197–217, <https://doi.org/10.1175/JPO-D-15-0008.1>, 2016.



- Tzortzis, R., Doglioli, A. M., Barrillon, S., Petrenko, A. A., d'Ovidio, F., Izard, L., Thyssen, M., Pascual, A., Barceló-Llull, B., Cyr, F., Tedetti, M., Bhairy, N., Garreau, P., Dumas, F., and Gregori, G.: Impact of moderately energetic fine-scale dynamics on the phytoplankton community structure in the western Mediterranean Sea, *Biogeosciences*, 18, 6455–6477, <https://doi.org/10.5194/bg-18-6455-2021>, 2021.
- 540 Tzortzis, R., Doglioli, A. M., Messié, M., Barrillon, S., Petrenko, A. A., Izard, L., Zhao, Y., d'Ovidio, F., Dumas, F., and Gregori, G.: The contrasted phytoplankton dynamics across a frontal system in the southwestern Mediterranean Sea, *Biogeosciences*, 20, 3491–3508, <https://doi.org/10.5194/bg-20-3491-2023>, 2023.
- Uitz, J., Stramski, D., Gentili, B., D'Ortenzio, F., and Claustre, H.: Estimates of phytoplankton class-specific and total primary production in the Mediterranean Sea from satellite ocean color observations, *Global Biogeochemical Cycles*, 26, <https://doi.org/10.1029/2011GB004055>, 2012.
- 545 Watson, J. R., Fuller, E. C., Castruccio, F. S., and Samhuri, J. F.: Fishermen Follow Fine-Scale Physical Ocean Features for Finance, *Frontiers in Marine Science*, 5, <https://doi.org/10.3389/fmars.2018.00046>, 2018.
- Xing, Q., Yu, H., and Wang, H.: Global mapping and evolution of persistent fronts in Large Marine Ecosystems over the past 40 years, *Nature Communications*, 15, 4090, <https://doi.org/10.1038/s41467-024-48566-w>, 2024.
- 550 Yang, K., Meyer, A., Strutton, P. G., and Fischer, A. M.: Global trends of fronts and chlorophyll in a warming ocean, *Communications Earth & Environment*, 4, 489, <https://doi.org/10.1038/s43247-023-01160-2>, 2023.